



## Characterization of the catalytic and kinetic properties of a thermostable *Thermoplasma acidophilum* $\alpha$ -glucosidase and its transglucosylation reaction with arbutin

Seong-Hwa Seo<sup>a</sup>, Kyoung-Hwa Choi<sup>a</sup>, Sungmin Hwang<sup>a</sup>, Jieun Kim<sup>a</sup>, Cheon-Seok Park<sup>b</sup>, Jung-Rae Rho<sup>c</sup>, Jaeho Cha<sup>a,\*</sup>

<sup>a</sup> Department of Microbiology, College of Natural Sciences, Pusan National University, Busan 609-735, Republic of Korea

<sup>b</sup> Graduate School of Biotechnology, and Institute of Life Science and Resources, KyungHee University, Yongin 446-701, Republic of Korea

<sup>c</sup> Department of Oceanography, Kunsan National University, Jeonbuk 573-701, Republic of Korea

### ARTICLE INFO

#### Article history:

Received 16 February 2011

Received in revised form 11 July 2011

Accepted 11 July 2011

Available online 20 July 2011

#### Keywords:

GH31  $\alpha$ -glucosidase

Hyperthermophiles

Thermostability

*Thermoplasma acidophilum*

Transglucosylation

### ABSTRACT

The gene (Ta0298) encoding a putative  $\alpha$ -glucosidase from hyperthermophilic archaeon *Thermoplasma acidophilum* (AglA) was cloned and expressed in *Escherichia coli*. Gel filtration chromatography of the purified enzyme indicated that the native form was a pentamer with strong maltose ( $\alpha$ -1,4 linkage)-hydrolyzing activity. AglA was optimally active at pH 5–6 and 80 °C and had a half-life of 16.8 h and 1.4 h at 80 °C and 85 °C, respectively. The enzyme also hydrolyzes kojibiose ( $\alpha$ -1,2), nigerose ( $\alpha$ -1,3), and isomaltose ( $\alpha$ -1,6) to a lesser extent. Analysis of the reaction with maltooligosaccharides and panose as substrates show that AglA specifically liberates glucose from the non-reducing end indicating that it is typical of a glycoside hydrolase family 31 (GH31)  $\alpha$ -glucosidase. Kinetic analyses revealed that the hydrolytic activity of AglA was greatly affected by the chain length of the substrate and the regiospecificity of the glucosidic linkages. The enzyme showed highest specificity for maltose and decreasing values of catalytic efficiency ( $k_{cat}/K_m$ ) toward higher maltooligosaccharides, although these still serve as substrates. The inhibition profile of AglA toward aesculin was revealed to be a mixed type of noncompetitive inhibition with a  $K_i$  value of 4.30  $\mu$ M and  $K'_i$  of 12.5  $\mu$ M, whereas that toward acarbose showed a competitive inhibition pattern with a  $K_i$  of 2.99  $\mu$ M. Structural analyses of two arbutin transglucosylation products using NMR indicated that the glucose unit of maltose was transferred to the C-3 and C-6 position in the glucose moiety of arbutin.

© 2011 Elsevier B.V. All rights reserved.

### 1. Introduction

$\alpha$ -Glucosidases (EC 3.2.1.20) are a widespread group of enzymes that catalyze the hydrolysis of the  $\alpha$ -glucosidic bond from the non-reducing end of a chain as well as the  $\alpha$ -glucosidic bond of free disaccharides [1,2]. With a high concentration of substrate, the enzyme also displays a transferring reaction (transglucosylation) to yield maltooligosaccharides [3,4]. Commercially available oligosaccharides, comprising an isomaltosyl or nigerosyl structure, are produced by  $\alpha$ -glucosidase-catalyzed transferring reactions [5,6]. The application of these enzymes in the biosynthesis of bioactive compounds using the transglucosylation activity is rapidly attract-

ing considerable interest due to the advantages of the specificity, efficiency, and safety of enzymatic reaction [5,7].

$\alpha$ -Glucosidases found in various organisms show diverse substrate specificities. Glycoside hydrolase family 13 (GH13) enzymes show considerably more activity toward heterogeneous substrates than to homogeneous substrates (i.e. maltooligosaccharides), whereas GH31 enzymes hydrolyze homogeneous substrates more rapidly than heterogeneous substrates. In prokaryotes, GH31 enzymes play an important role in nutrient uptake and utilization [8]. Although a number of  $\alpha$ -glucosidases belonging to the GH31 family have been isolated from bacteria, relatively few are known from the archaea. Due to their inherent thermostability, hyperthermophilic  $\alpha$ -glucosidases isolated from archaea have great potential for the biosynthesis of bioactive glycosides. These hyperthermophilic  $\alpha$ -glucosidases can catalyze reactions at high temperatures with higher substrate concentrations, lower viscosity, fewer risks of microbial contamination, and often higher reaction rates [9,10]. The previously characterized archaeal representatives are the enzymes from *Sulfolobus solfataricus* [11,12],

\* Corresponding author at: Department of Microbiology, College of Natural Sciences, Pusan National University, San 30, Jangjeon-dong, Geumjeong-gu, Busan 609-735, Republic of Korea. Tel.: +82 51 510 2196; fax: +82 51 514 1778.

E-mail address: [jhcha@pusan.ac.kr](mailto:jhcha@pusan.ac.kr) (J. Cha).

*Pyrococcus furiosus* [13], *Thermococcus* sp. [14], and *Picrophilus torridus* [15]. Among these, only *S. solfataricus* and *P. torridus*  $\alpha$ -glucosidases have been produced recombinantly [16–18]. There has been a constant effort to discover a functional, thermostable  $\alpha$ -glucosidase with industrial potential. The archaeal genome was scanned for genes encoding GH31  $\alpha$ -glucosidase and a putative  $\alpha$ -glucosidase gene (*aglA*) from *Thermoplasma acidophilum* DSM 1728 was chosen. This *aglA* gene was cloned and expressed to study the catalytic properties of the gene product. Herein, we show that the putative  $\alpha$ -glucosidase of *T. acidophilum* is indeed a thermo- and acidophilic  $\alpha$ -glucosidase that has specific  $\alpha$ -1,3 and  $\alpha$ -1,6-transferring activities as well as hydrolytic activity.

## 2. Materials and methods

### 2.1. Cloning and expression of the gene encoding AglA

Genomic DNA of *T. acidophilum* DSM 1728 was obtained from Prof. Sang-Hyeon Lee (Silla University, Busan, Korea). Cloning of the *T. acidophilum* ORF Ta0298 was accomplished by amplifying the genomic region surrounding the *aglA* gene with primers TA-NdeI-FP (5'-CATATGCTTGACGATATCCGAGGTTTATGAAT-3') and TA-XhoI-RP (5'-CTCGAGCTTCAACCTTATTATGCCATCG-3') using the genomic DNA as the template. The 2270-bp product was cloned into a pGEM-T vector using a T-vector cloning kit (Promega). The vector obtained (pGEM-*aglA*) was digested with *NdeI* and *XhoI* and ligated with pET29b (Novagen) that had been digested with the same restriction enzymes. After sequence analysis, one clone containing no PCR errors was selected and designated pET-TAAGL, and this was used for the production of a six histidine-tagged target enzyme.

### 2.2. Purification of the recombinant AglA

The recombinant *Escherichia coli* BL21(DE3) carrying pET-TAAGL was cultured in Luria-Bertani broth [1% (w/v) Bacto-tryptone, 0.5% (w/v) yeast extract, 0.5% (w/v) NaCl] supplemented with kanamycin (30  $\mu$ g/mL) overnight at 37 °C, and 1 mL of cells was transferred to 1 L fresh medium and cultured at 30 °C until an OD<sub>600nm</sub> of between 0.6 and 0.8 was reached. At this point, protein expression was induced by the addition of 0.1 mM isopropyl  $\beta$ -D-1-thiogalactopyranoside (IPTG). After 6 h of induction, the cells were harvested by centrifugation (10,000  $\times$  g, 20 min, 4 °C) and resuspended in 20 mM sodium phosphate buffer (pH 7.0). Cells were disrupted by a two-fold passage through a French pressure cell (American Instruments, Silver Spring, MD). The crude cell extract was centrifuged at 12,000  $\times$  g (20 min, 4 °C) to remove cell debris. The supernatant was then incubated at 70 °C for 30 min to denature thermolabile host proteins and centrifuged again at 12,000  $\times$  g (20 min, 4 °C) to remove denatured proteins from the extract. The resulting supernatant was dialyzed against 20 mM sodium phosphate buffer (pH 7.0) and 0.5 M NaCl at 4 °C overnight and subjected to nickel-nitrilotriacetic acid (Ni-NTA) affinity chromatography (Qiagen, Hilden, Germany) using the same equilibration buffer. The bound proteins were eluted out using 100 mM imidazole in the same buffer at a flow rate of 1.0 mL/min. The protein solution was concentrated using a Centricon-10 filter from Amicon (Millipore, Bedford, MA) and dialyzed using Spectra/Por molecular porous membrane tubing (Spectrum Laboratories, Rancho Dominguez, USA) against 20 mM sodium phosphate buffer (pH 7.0). The molecular mass of the native enzyme was estimated by gel filtration chromatography using a Sephacryl S-300 HR 16/60 column equilibrated with 20 mM sodium phosphate (pH 7.0), 150 mM NaCl. The purity of the recombinant AglA was checked by SDS-PAGE using a 12% (w/v) gel. The protein concentration was determined according to the Bradford method, using bovine serum albumin as a stan-

dard [19]. An extinction coefficient at 280 nm of 136,140 M<sup>-1</sup> cm<sup>-1</sup> was determined for the purified enzyme. Determination of the subsequent protein concentration was based on the absorbance at 280 nm.

### 2.3. Enzyme assay

The enzyme activity was determined using *p*-nitrophenyl- $\alpha$ -D-glucopyranoside (pNPG; Sigma–Aldrich). The reaction mixture, containing 0.5 mM pNPG, 25 mM sodium acetate buffer (pH 5.5), and enzyme in a total volume of 200  $\mu$ L, was incubated at 80 °C for 5 min. The enzymatic reaction was terminated by the addition 100  $\mu$ L of 1 M Na<sub>2</sub>CO<sub>3</sub>, and the *p*-nitrophenol liberated was measured at 415 nm. The influence of pH on the activity of AglA was measured at 80 °C in sodium citrate (pH 4.0–4.5), sodium acetate (pH 4.5–6.0), MES (pH 5.5–7.0), and HEPES (pH 6.5–8.5) buffers. The pH of each buffer system was adjusted at 80 °C using the standard enzyme assay conditions described above. The influence of temperature on the activity of AglA was determined at a constant pH of 5.5 using 25 mM sodium acetate buffer (pH 5.5), and temperatures ranging from 40 to 100 °C were studied. The thermostability of the enzyme was analyzed by incubating the enzyme (1  $\mu$ g) at 75, 80, 85, or 90 °C. Aliquots were taken at hourly interval and placed immediately in an ice-water bath to halt the enzymatic activity. The residual activities of the aliquots were measured with 0.5 mM pNPG under standard conditions. One unit of the enzyme activity was defined as the amount of enzyme that releases 1  $\mu$ mol of *p*-nitrophenol per minute.

The effects of various metal ions and chemical reagents on AglA activity were examined after preincubation of the purified enzyme with metal ions or other reagents at 1 mM concentration at 80 °C for 5 min. The activity assayed in the absence of metal ions or reagents was taken to be 100%. The activity with natural substrates were analyzed by thin-layer chromatography (TLC) on Whatman K6F silica gel plates (Whatman, Maidstone, UK) using 1-butanol/ethanol/H<sub>2</sub>O (5:5:3, v/v/v) as the mobile phase as described previously [20].

The enzyme activity with natural substrates was measured quantitatively by determining the amounts of glucose released after enzyme treatment. The reaction mixtures (100  $\mu$ L) containing 10 mM substrate were incubated with 0.5  $\mu$ g of purified enzyme for 5 min. The reaction was stopped by the addition of 200  $\mu$ L of 12 N H<sub>2</sub>SO<sub>4</sub>, and 200  $\mu$ L of glucose oxidase assay reagent (Sigma) was added to the stopped reaction. Aliquots of 200  $\mu$ L that were transferred to a 96-well plate were developed for 30 min, and absorbance was measured at 490 nm to determine the amount of glucose produced by enzyme activity in the reaction. One unit of the enzyme activity was defined as the amount of the enzyme that hydrolyzes the substrate to release 1  $\mu$ mol of the respective product per minute. All reactions were performed in triplicate.

### 2.4. Kinetic parameters

The kinetic parameters of recombinant AglA were determined using the glucose oxidase assay to follow the production of glucose upon the addition of enzyme (0.15  $\mu$ g) at increasing concentrations (0.1–4.0 mM) of substrates, such as maltose, maltotriose, maltotetraose, isomaltose, kojibiose, panose, and pNPG, with a reaction time of 6 min. Reactions were linear within this time frame. The program Sigmaplot was used to fit the data to the Michaelis–Menten equation and estimate the kinetic parameters, *K*<sub>m</sub> and *V*<sub>max</sub>, of the enzyme. All experiments were performed in triplicate. *K*<sub>i</sub> values for aesculin and acarbose were determined by measuring the rate of maltose hydrolysis by AglA at varying inhibitor concentrations (1–20  $\mu$ M). Inhibition types for the inhibitors were determined by Lineweaver–Burk plot.

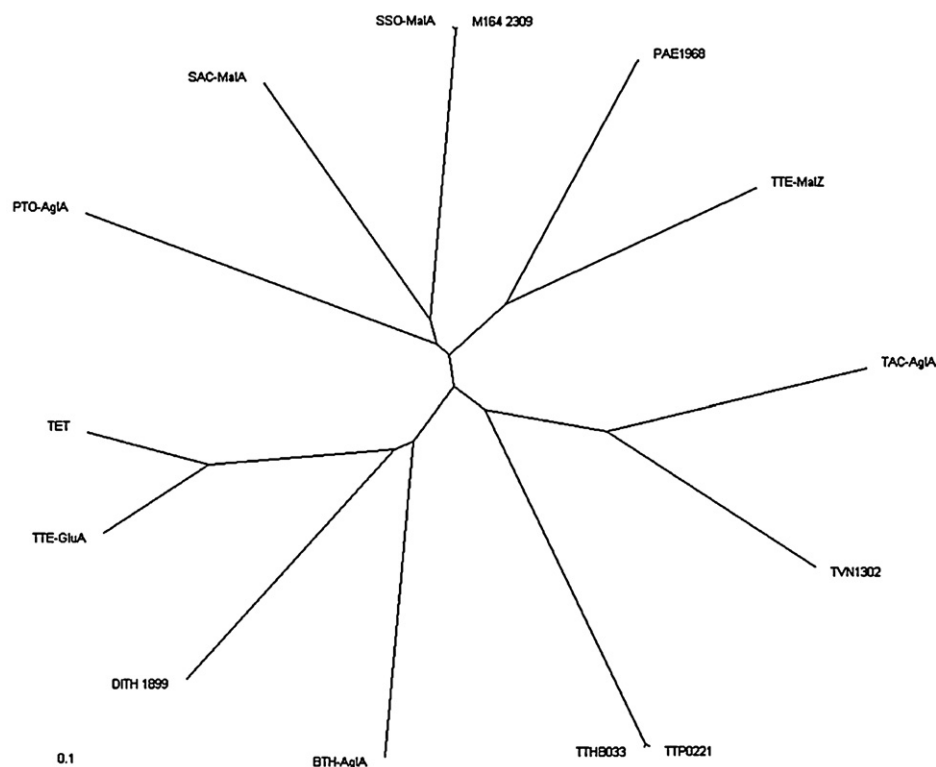


**Fig. 1.** Phylogenetic tree of selected members of glycoside hydrolase family 31. Phylip format tree outputs from the CLUSTAL X analysis were visualized with TreeViewPPC based on the distance matrix using the neighbor-joining method. The bar at the lower left corner indicates the substitution rate (substitution/site). The following abbreviations are used (accession numbers are in parentheses): TAC-AglA, *T. acidophilum* AglA (CAC11443); TVN1302, *Thermoplasma volcanium* GSS1 TVN1302 (BAB60467); SSO-MaIA, *S. solfataricus* P2 MaIA (AAK43151); SAC-MaIA, *S. acidophilus* MaIA (AAY80507); M164.2309, *Sulfolobus islandicus* M.16.4  $\alpha$ -glucosidase (ACR42908); PTO-AglA, *Picrophilus torridus* AglA (AAT42677); PAE1968, *Pyrobaculum aerophilus* str. IM2, PAE1968 (AAL63848); TTE-MaIZ, *Thermoproteus tenax* MaIZ (CAF18491); TTE-GluA, *Thermoanaerobacter tengcongensis* MB4 GluA (AAM23323); TET, *Thermoanaerobacter ethanolicus*  $\alpha$ -glucosidase (ABR26230); DITH.1899, *Dictyoglomus thermophilum*  $\alpha$ -glucosidase; BTH-AglA, *Bacillus thermoamyloliquefaciens* AglA (BAA76396); TTHB033, *Thermus thermophilus* HB8  $\alpha$ -glucosidase; and TTP0221 (BAD71829), *Thermus thermophilus* HB27  $\alpha$ -glucosidase (AAS82549).

## 2.5. Transglucosylation reaction and purification of arbutin derivatives

The transglucosylation activity of AglA was investigated using various glycosides. The reaction (100  $\mu$ L) was carried out at 80 °C for 3 h with 25 mM maltose as donor and 25 mM arbutin, salicin, or polydatin as an acceptor, 1.5  $\mu$ g enzyme in 25 mM sodium acetate buffer (pH 5.5). The reaction products acquired by the transglucosylation reaction were collected, freeze-dried, and then concentrated. These products were analyzed by TLC and arbutin transfer products were purified by a recycling preparative HPLC (JAI Korea, Seoul, Korea) as described previously [21].

## 2.6. Matrix-assisted laser desorption/ionization time-of-flight mass spectrometry

The mass spectrum was acquired using a Voyager DE-STR matrix-assisted laser desorption/ionization time-of-flight (MALDI-TOF) mass spectrometer (Applied Biosystems, Foster City, CA) as described previously [22].

## 2.7. Nuclear magnetic resonance analysis

Approximately 5 mg of each purified compound was dissolved in 0.5 mL of deuterium oxide ( $D_2O$ ) and all NMR experiments were performed using a Varian VNMR5 500 spectrometer (Varian, Palo Alto, CA) at 23 °C. Chemical shifts of proton signals were referenced to a peak due to  $H_2O$  at 4.75 ppm and those of carbon signals to

the TSP internal standard. Complete spectral assignments of each compound were given on the basis of a combination of 1D and 2D NMR spectra (COSY, TOCSY, HSQC, and HMB).

## 3. Results

### 3.1. Phylogenetic analysis of *T. acidophilum* AglA

The gene (*aglA*; Ta0298) corresponding to a putative  $\alpha$ -glucosidase from *T. acidophilum* was amplified by PCR and the entire ORF was cloned and sequenced. The ORF encoded a protein comprising 749 amino acids with a predicted molecular mass of 85.9 kDa. No detectable signal peptide sequences were found in AglA as revealed by searches with the SignalP 3.0 program [23]. AglA was classified as a member of GH31 based on the conserved active site pattern [GF]-[LIVMF]-W-[HL]-D-M-[NSA]-E-P, which is characteristic of this family [Carbohydrate Active Enzymes database (<http://www.cazy.org>)]. In archaea, only two enzymes, *S. solfataricus* MaIA and *P. torridus* AglA, belonging to this family have been characterized [17,18]. *T. acidophilum* AglA showed 35% and 36% identity with *S. solfataricus* MaIA and *P. torridus* AglA, respectively. Fourteen thermostable GH31  $\alpha$ -glucosidase orthologs were compared by phylogenetic analysis. The results revealed that *T. acidophilum* AglA is more similar to orthologs from members of the bacterial genus *Thermus* than to sequences from members of the phylogenetically closely related archaeal genera *Picrophilus*, *Sulfolobus*, *Pyrobaculum*, and *Thermoproteus* (Fig. 1).

**Table 1**  
Purification step of recombinant AgIA.

|                   | Total protein (mg) | Total activity (U) | Specific activity (U/mg) | Yield (%) | Fold |
|-------------------|--------------------|--------------------|--------------------------|-----------|------|
| Cell-free extract | 196                | 961,000            | 4900                     | 100       | 1.0  |
| Heat treatment    | 15.7               | 683,000            | 43,500                   | 71        | 8.9  |
| Ni-NTA affinity   | 2.25               | 101,000            | 45,000                   | 11        | 9.2  |

### 3.2. Purification and enzyme properties of AgIA

The recombinant AgIA was expressed in *E. coli* BL21(DE3) cells. The enzyme was purified nine-fold by heat treatment of the crude cell-free extract for 30 min at 70 °C, followed by Ni-NTA affinity chromatography (Table 1). The apparent size of the purified recombinant AgIA enzyme estimated by SDS-PAGE was approximately 82 kDa, which is in good agreement with the size calculated from the primary structure (Fig. 2A). The molecular mass of AgIA was determined to be about 409 kDa by gel filtration chromatography, revealed that the AgIA is a pentamer in its active state (Fig. 2B). The pI value of the recombinant AgIA was estimated to 5.29 by Expasy ProtParam tool program (<http://ca.expasy.org/tools/protparam.html>).

The pH range at which AgIA was active was determined using pNPG as the substrate. AgIA was most active at pHs ranging from 5.0 to 6.0, and the optimum pH was found to be 5.5 (Fig. 3A). From the fact that the observed optimum pH range is close to the neutral region, it is evident that AgIA is an intracellular enzyme. High enzyme activities (>60%) were still maintained until pH 4.0, whereas the activity decreased sharply at pHs greater than 7.5. The optimal temperature for AgIA activity was 80 °C, and relatively low activities were observed below 50 °C and above 95 °C (Fig. 3B). The enzyme exhibited remarkable thermostability, retaining its full activity after 16.8 h incubation at 80 °C (Fig. 3C). The half-life of AgIA was determined to be 1.4 h at 85 °C and 12 min at 90 °C. This result implies that AgIA was successfully expressed in *E. coli*, and its thermostability preserved. The effects of metal ions and different reagents on enzyme activity were examined (Table 2).  $Mn^{2+}$ , as chloride salts at a concentration of 1 mM, slightly enhanced the enzyme activity; however,  $Cu^{2+}$  and  $Zn^{2+}$  reduced the activity to

**Table 2**  
Effects of metal ions and reagents on the activity of recombinant AgIA.

| Reagents                              | Concentration (mM) | Relative activity (%) |
|---------------------------------------|--------------------|-----------------------|
| None                                  |                    | 100                   |
| EDTA                                  | 1                  | 93 ± 3.3              |
| MgCl <sub>2</sub>                     | 1                  | 104 ± 0.5             |
| CaCl <sub>2</sub>                     | 1                  | 103 ± 2.4             |
| ZnCl <sub>2</sub>                     | 1                  | 28 ± 2.6              |
| NiCl <sub>2</sub>                     | 1                  | 84 ± 3                |
| CoCl <sub>2</sub>                     | 1                  | 105 ± 1.9             |
| MnCl <sub>2</sub>                     | 1                  | 159 ± 0.4             |
| CuCl <sub>2</sub>                     | 1                  | 35 ± 2.9              |
| HgCl <sub>2</sub>                     | 1                  | 4.2 ± 0.4             |
| Dithiothreitol                        | 1                  | 107 ± 0.7             |
| 2-Mercaptoethanol                     | 1                  | 108 ± 2.7             |
| SDS                                   | 1                  | ND <sup>a</sup>       |
| N-Bromosuccinimide                    | 1                  | 7.8 ± 1.9             |
| p-Chloromercuribenzoic acid           | 1                  | 95 ± 0.7              |
| Dimethylaminopropyl ethylcarbodiimide | 1                  | 107 ± 0.3             |

The enzyme was preincubated with the above reagents at 80 °C for 5 min. Aliquots were tested for AgIA activity by incubating the samples with 0.5 mM pNPG in 25 mM sodium acetate buffer (pH 5.5) at 80 °C for 5 min. The metal ions and other reagents were added at a final concentration of 1 mM except for SDS (1%). The relative values shown are the percentages of the activity without additives.

<sup>a</sup> ND, not detected.

34.9 and 28% of control levels, respectively, while  $Hg^{2+}$  and N-bromosuccinimide strongly inhibited the enzyme. Additionally, the activity of enzyme was completely inactivated by SDS.

The substrate specificity of the enzyme was examined with various types of  $\alpha$ -glucans, including di- and oligomaltosaccharides. Broad specificity was observed for the linkages of the glycosidic

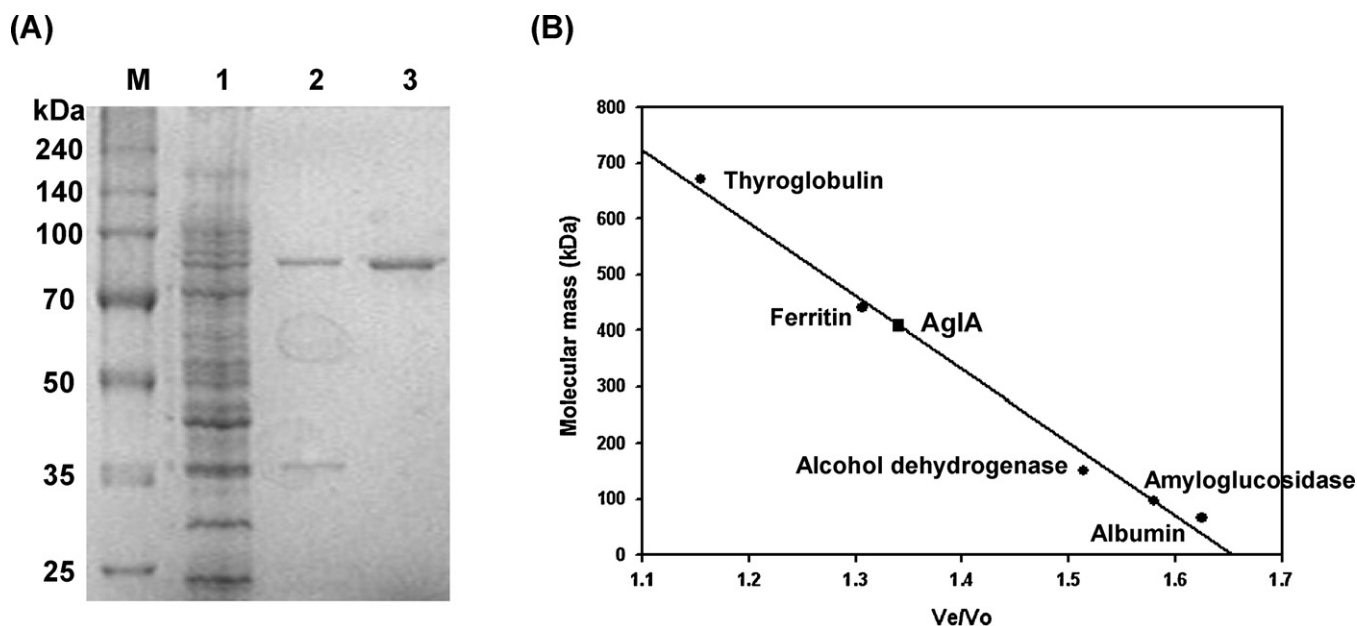


**Fig. 2.** SDS-PAGE (A) and molecular mass determination (B) of AgIA. Lane M, protein size standards; lane 1, cell-free extracts of recombinant AgIA; lane 2, proteins after heat treatment; lane 3, proteins after Ni-NTA affinity chromatography. Molecular mass of the native enzyme was estimated by gel filtration chromatography using Sephacryl S-300 HR 16/60 column. The column was calibrated with molecular mass standards: thyroglobulin (670 kDa), ferritin (440 kDa), alcohol dehydrogenase (150 kDa), amyloglucosidase (97 kDa), and albumin (66 kDa).



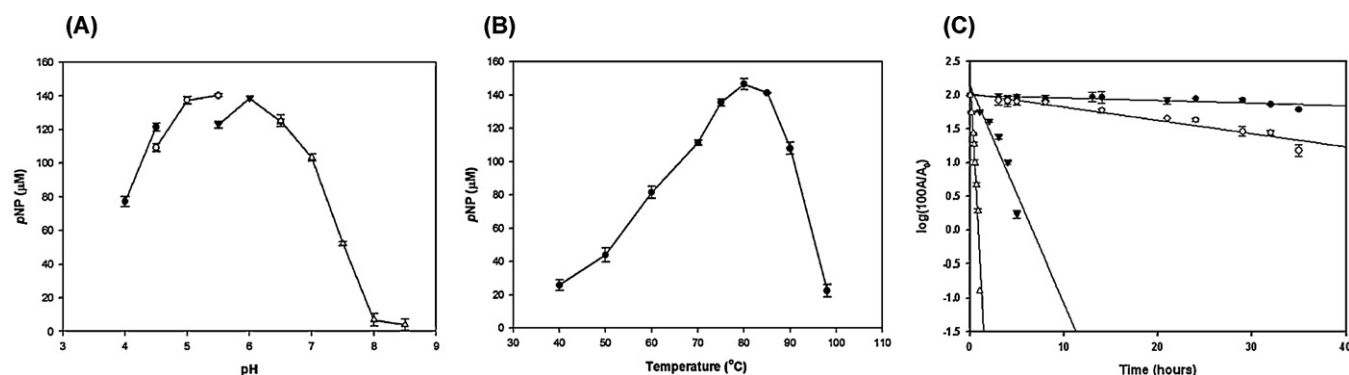


**Fig. 3.** Effects of pH and temperature on the activity and stability of AgIA. (A) The activity was determined at 80  $^{\circ}\text{C}$  for 5 min with pNPG in various 25 mM buffer systems: for pH 4.0–4.5, sodium citrate (●); for pH 4.5–5.5, sodium acetate (○); for pH 5.5–6.5, MES (▼); for pH 6.5–8.5, HEPES (△). (B) The effect of temperature on enzyme activity was determined at temperatures ranging from 40  $^{\circ}\text{C}$  to 98  $^{\circ}\text{C}$  at the optimum pH of 5.5. (C) To determine the thermostability of AgIA, the enzyme was heated at 75  $^{\circ}\text{C}$  (●), 80  $^{\circ}\text{C}$  (○), 85  $^{\circ}\text{C}$  (▼), and 90  $^{\circ}\text{C}$  (△) in 25 mM sodium acetate buffer (pH 5.5). After various time intervals, samples were withdrawn and the residual activity was measured at 80  $^{\circ}\text{C}$  for 5 min with pNPG. Error bars represent the standard deviation from three separate experiments.

**Table 3**  
Substrate specificity of recombinant AgIA.

| Substrate      | Glycosidic linkage  | Glucose released ( $\mu\text{mol}/\text{min } \mu\text{g protein}^{-1}$ ) <sup>a</sup> |
|----------------|---|--|
| Trehalose      | $\alpha\text{-D-Glc-(1} \rightarrow 1\text{)-D-Glc}$  | ND <sup>c</sup>  |
| Kojibiose      | $\alpha\text{-D-Glc-(1} \rightarrow 2\text{)-D-Glc}$  | 445 <sup>b</sup>   |
| Nigerose       | $\alpha\text{-D-Glc-(1} \rightarrow 3\text{)-D-Glc}$  | 233  |
| Maltose        | $\alpha\text{-D-Glc-(1} \rightarrow 4\text{)-D-Glc}$  | 582  |
| Isomaltose     | $\alpha\text{-D-Glc-(1} \rightarrow 6\text{)-D-Glc}$  | 153  |
| Cellobiose     | $\beta\text{-D-Glc-(1} \rightarrow 4\text{)-D-Glc}$   | ND   |
| Panose         | $\alpha\text{-D-Glc-(1} \rightarrow 6\text{)-}\alpha\text{-D-Glc-(1} \rightarrow 4\text{)-D-Glc}$   | 136  |
| Isomaltotriose | $\alpha\text{-D-Glc-(1} \rightarrow 6\text{)-}\alpha\text{-D-Glc-(1} \rightarrow 6\text{)-D-Glc}$   | 4 <sup>b</sup>   |
| Maltotriose    | $\alpha\text{-D-Glc-(1} \rightarrow 4\text{)-}\alpha\text{-D-Glc-(1} \rightarrow 4\text{)-D-Glc}$   | 378  |
| Maltotetraose  | $\alpha\text{-D-Glc-(1} \rightarrow 4\text{)-}\alpha\text{-D-Glc-(1} \rightarrow 4\text{)-}\alpha\text{-D-Glc-(1} \rightarrow 4\text{)-D-Glc}$  | 317  |
| Maltopentaose  | $\alpha\text{-D-Glc-(1} \rightarrow 4\text{)-}\alpha\text{-D-Glc-(1} \rightarrow 4\text{)-}\alpha\text{-D-Glc-(1} \rightarrow 4\text{)-}\alpha\text{-D-Glc-(1} \rightarrow 4\text{)-D-Glc}$ | 287  |

<sup>a</sup> Activity was determined with 0.5  $\mu\text{g}$  of pure enzyme and 10 mM of each substrate at 80  $^{\circ}\text{C}$  for 5 min, except where indicated otherwise.

<sup>b</sup> Activity was determined with 0.5  $\mu\text{g}$  of pure enzyme and 1 mM substrate at 80  $^{\circ}\text{C}$  for 5 min.

<sup>c</sup> ND, not detected.

bond. AgIA showed the highest activity with maltose ( $\alpha$ -1,4 bond), though it also hydrolyzed kojibiose ( $\alpha$ -1,2), nigerose ( $\alpha$ -1,3), and isomaltose ( $\alpha$ -1,6) with lower efficiencies (Table 3). In contrast, cellobiose, which has  $\beta$ -linked glycosidic bond, was not hydrolyzed by AgIA. From the kinetic results of AgIA with maltooligosaccharides, the rate of maltooligosaccharide hydrolysis decreased with an increasing number of glucose units in the substrate (Table 4). The decreased hydrolytic activities of AgIA toward longer maltooligosaccharides were due to the lower  $k_{\text{cat}}$  values than that of maltose. The observed enzymatic activity with maltotetraose was approximately half of that with maltose. The low catalytic efficiency of AgIA against isomaltose, panose, and pNPG, which have  $\alpha$ -1,6 glycosidic linkages, was due to the high  $K_{\text{m}}$  and low  $k_{\text{cat}}$  values.

TLC analyses of the reaction products of AgIA with oligosaccharides showed that glucose was initially released when maltooligosaccharides with different chain lengths were used as substrates and that the hydrolysis of panose yielded glucose and maltose, implying that the enzyme hydrolyzes the maltooligosac-

charides in an exo-acting manner from the non-reducing end (Fig. 4). These hydrolysis patterns indicate that AgIA is a typical GH31-type  $\alpha$ -glucosidase. The overall characteristics of AgIA were summarized in Table 5.

### 3.3. Inhibition profile of AgIA

The effectiveness of  $\alpha$ -glucosidase inhibitors on AgIA was tested using maltose as a substrate in the presence of aesculin and acarbose, the known inhibitor. The inhibition constants ( $K_i$ ) of aesculin and acarbose against AgIA were determined using the glucose oxidase assay with maltose as a substrate. Lineweaver-Burk plot for AgIA in the presence of aesculin and acarbose, respectively, indicates the type of inhibition produced by acarbose and aesculin. The inhibition constants  $K_i$  and  $K_i'$  represent the respective dissociation constants of the enzyme-inhibitor complex (EI) and the enzyme-substrate-inhibitor complex (ESI). Aesculin inhibition was demonstrated to be a mixed type of noncompetitive inhibition with a  $K_i$  value of 4.30  $\mu\text{M}$  and a  $K_i'$  of 12.5  $\mu\text{M}$ , whereas acarbose showed a competitive inhibition pattern with a  $K_i$  of 2.99  $\mu\text{M}$  (Table 6).

### 3.4. Transglucosylation activity of AgIA

The transglucosylation activity of AgIA was investigated using arbutin, salicin, and polydatin as an acceptor and maltose as a donor, respectively. The reaction was allowed to proceed for 3 h before analysis by TLC. Four distinct transglucosylation products, two with maltose-transferred products (MG1 and MG2) and the other two with acceptor-transferred products (A1 and A2) were

**Table 4**  
Kinetic parameters of recombinant AgIA.

| Substrate     | $K_{\text{m}}$ (mM) | $k_{\text{cat}}$ ( $\text{s}^{-1}$ ) | $k_{\text{cat}}/K_{\text{m}}$ ( $\text{mM}^{-1} \text{s}^{-1}$ ) |
|---------------|---------------------|--------------------------------------|--|
| Maltose       | 0.65                | 143                                  | 220  |
| Maltotriose   | 0.47                | 90.2                                 | 194  |
| Maltotetraose | 0.67                | 85.5                                 | 128  |
| Isomaltose    | 4.25                | 22.9                                 | 5.4  |
| Kojibiose     | 1.24                | 127                                  | 103  |
| Panose        | 6.60                | 35.9                                 | 5.4  |
| pNPG          | 1.77                | 59.7                                 | 33.7   |

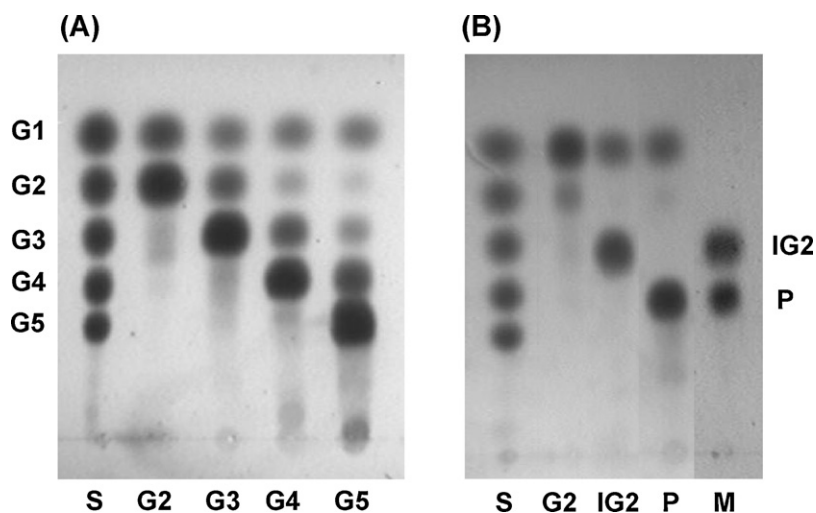


**Fig. 4.** TLC analysis of the products of AgIA hydrolysis. The reaction was carried out at 80 °C for 5 min with maltooligosaccharides (A) and for 30 min with maltose, isomaltose, and panose (B). Lane S, standard markers from G1 (glucose) to G5 (maltopentaose); lane M, IG2 (isomaltose) and P (panose).

**Table 5**  
Characteristics of recombinant AgIA.

| Substrate | Optimum pH | Optimum temperature (°C) | $K_m$ (mM) | $k_{cat}$ ( $s^{-1}$ ) | $k_{cat}/K_m$ ( $mM^{-1} s^{-1}$ ) | Half-life ( $t_{1/2}$ )         |
|-----------|------------|--------------------------|------------|------------------------|------------------------------------|---------------------------------|
| pNPG      | 5.5        | 80                       | 1.77       | 59.7                   | 33.7                               | 1.4 h (85 °C)<br>12 min (90 °C) |

observed (Fig. 5A). In case of arbutin, an arbutin transfer product (AG2) was formed early (within 5 min) and rapidly decreased with an increase in reaction time, whereas AG1 was produced later and retained at 2 h (Fig. 5B). The maximum yields of AG1 and AG2 estimated by densitometry were approximately 30% and 26%, respectively. AG1 and AG2 were purified using recycling preparative HPLC. The isolated AG1 and AG2 appeared as single spots on TLC (Fig. 5C, lanes 17 and 18). Two compounds showed the same molecular ion peaks at  $m/z$  457  $[M+Na]^+$  by MALDI-TOF/MS analysis, indicating that the products consisted of a glucose unit and arbutin. This finding was also supported by two characteristic anomeric protons, crowded protons in the range of 3.2–4.0 ppm, and two downfield-shifted doublets in the  $^1H$  NMR spectrum. Furthermore, each anomeric proton in AG1 and AG2 was recognized as  $\alpha$  and  $\beta$  positions from the coupling constant values ( $J=7.8$  and  $3.7$  Hz, respectively). However, the chemical shift of the  $\beta$ -positioned anomeric proton in the two compounds was different. This suggested a difference in the linkage of the glucose unit to the arbutin moiety. At first, all proton and carbon assignments in the two glucose units were made by the COSY, TOCSY, and HSQC experiments to determine the connectivity between the glucose unit and arbutin. In AG1, the  $\beta$  anomeric proton at 4.88 ppm (C-1'') in the glucose unit showed a correlation with the carbon at 65.7 ppm (C-6') in arbutin in the HMBC spectrum, indicating a  $\alpha$ -Glc [1  $\rightarrow$  6]- $\beta$ -Glc linkage. On the other hand, AG2 showed an

HMBC correlation of the  $\beta$  anomeric proton at 5.30 ppm (C-1'') in the glucose unit with the carbon at 81.7 ppm (C-3') in arbutin. This presents the  $\alpha$ -Glc [1  $\rightarrow$  3]- $\beta$ -Glc linkage. Accordingly, AG1 and AG2 were established as  $\alpha$ -D-glucosyl-(1,6)-arbutin, and  $\alpha$ -D-glucosyl-(1,3)-arbutin, respectively (Fig. 5D).

#### 4. Discussion

The purpose of this study was to discover an  $\alpha$ -glucosidase that has industrial potential. Extremely thermophilic  $\alpha$ -glucosidases, which have strong transglycosylation activity, are ideal for application to the synthesis of functional oligosaccharides, isomaltooligosaccharides and conjugate sugars [24–26]. For the production of isomaltooligosaccharides,  $\alpha$ -amylase and  $\beta$ -amylase together with  $\alpha$ -glucosidase are required. Thermostable enzymes are advantageous because the liquefaction of starch by  $\alpha$ -amylase is considerably faster and gives high yields at higher temperatures. Therefore, thermostable  $\alpha$ -glucosidases, isolated from a variety of thermophiles or hyperthermophiles, are potential candidates for improvements in isomaltooligosaccharide production and are a superior replacement for *Aspergillus niger*  $\alpha$ -glucosidase, which is used commercially. Thermostable  $\alpha$ -glucosidases have previously been characterized from bacteria and archaea [11–15,27,28]; however, the transglycosylation properties of these enzymes are not well defined, particularly in the archaea.

**Table 6**  
Acarbose inhibition pattern of  $\alpha$ -glucosidase related enzymes from various sources.

| Enzyme  | Type of inhibition   | $K_i^a$ ( $\mu M$ ) | $K_i'^b$ ( $\mu M$ ) |
|---|----------------------|---------------------|----------------------|
| AgIA (archaeal $\alpha$ -glucosidase)             | Competitive          | $2.99 \pm 0.02$     |                      |
| Yeast $\alpha$ -glucosidase <sup>c</sup>          | Competitive          | $77.9 \pm 11.4$     |                      |
| Rat intestine $\alpha$ -glucosidase <sup>c</sup>  | Competitive          | $0.06 \pm 0.006$    |                      |
| <i>Bacillus</i> CGTase <sup>c</sup>               | Mixed noncompetitive | $2.53 \pm 0.30$     | $3.09 \pm 0.25$      |
| Porcine pancreatic $\alpha$ -amylase <sup>c</sup> | Mixed noncompetitive | $0.64 \pm 0.20$     | $0.64 \pm 0.06$      |

<sup>a</sup> $K_i$  is the inhibition constant, defined as  $[E][I]/[EI]$ .

<sup>b</sup> $K_i'$  is the inhibition constant, defined as  $[EI][S]/[ESI]$ .

<sup>c</sup>Data from Ref. [35].

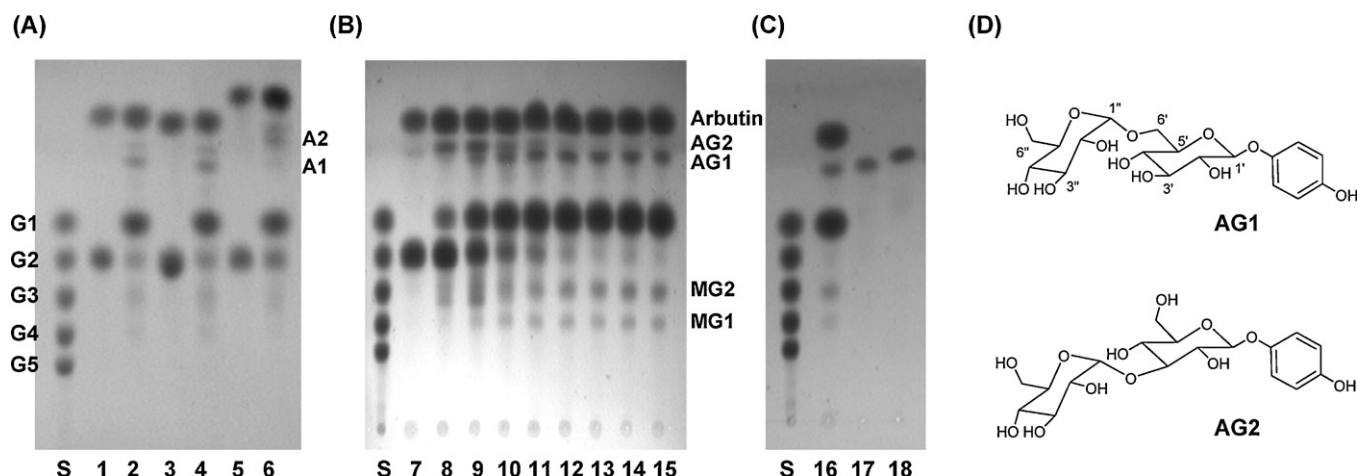


**Fig. 5.** Identification of the transglucosylation products of AgIA with various acceptors. (A) TLC analysis of the arbutin, salicin, and polydatin transglucosylation products. (B) TLC analysis of the arbutin transglucosylation products as a function of time. Lane S, standard markers from G1 (glucose) to G5 (maltopentaose); lane 1, maltose and arbutin; lane 2, reaction products of maltose and arbutin; lane 3, maltose and salicin, lane 4, reaction products of maltose and salicin, lane 5, maltose and polydatin, lane 6, reaction products of maltose and polydatin, lanes 7–15, reaction products at different reaction times (0, 5, 30, 60, 90, 120, 150, 180, and 240 min, respectively). A1, acceptor product 1; A2, acceptor product 2; AG1, arbutin transglucosylation product 1; AG2, arbutin transglucosylation product 2; MG1, maltose transglucosylation product 1; MG2, maltose transglucosylation product 2. (C) The transglucosylation products AG1 and AG2 purified by preparative recycling HPLC. Lane 16, reaction products of the arbutin transglucosylation; lane 17, purified AG1; lane 18, purified AG2. (D) The molecular structures of arbutin transglucosylation products AG1 and AG2.

We cloned and expressed the *T. acidophilum*  $\alpha$ -glucosidase in *E. coli*. The size of the *T. acidophilum*  $\alpha$ -glucosidase and the multimeric quaternary structure resembles those of other GH31  $\alpha$ -glucosidases [18,29]. The closer relationship of the AgIA with bacterial *Thermus* enzymes than phylogenetically related archaeal enzymes based on phylogenetic analysis implies that horizontal gene transfer has occurred between bacteria and archaea. This is consistent with the phylogenetic allocation of the *P. torridus* AgIA sequence and supports the hypothesis that there could have been a gene transfer event [18]. The temperature and pH profiles of AgIA and its remarkable resistance to thermal inactivation at temperatures up to 85 °C (half-life at this temperature, >1 h) are in agreement with the high optimal growth conditions of *T. acidophilum*.

AgIA acts as a typical GH31  $\alpha$ -glucosidase, removing a single D-glycosyl group from the non-reducing end of maltooligosaccharides. The rate of enzyme hydrolysis is affected by substrate molecular size and structure, and also by the next bond in sequence. It preferentially hydrolyzes maltose. The hydrolysis rate increases with a decrease in the chain length of the substrate. AgIA has a broad specificity as it is able to attack any glycosidic linkage of disaccharides, but the rate of hydrolysis of  $\alpha$ -1,4 linkages is higher than that of other linkages. It is quite distinguishable from renarchoal glucoamylases in that the rates of hydrolysis of non-reducing  $\alpha$ -1,4 bonds decrease with the increase in the molecular mass of the substrate up to maltopentaose [30]. AgIA has higher substrate specificity for smaller molecules such as maltose than for the maltooligosaccharides. The hydrolysis of  $\alpha$ -1,6-linked substrates, isomaltose and panose, but not isomaltotriose, was observed and indicates that the enzyme is only able to hydrolyze small  $\alpha$ -1,6-linked substrates. The apparent activity against pNPG indicates a lack of discrimination for glycosyl moieties in disaccharide substrates.

It has been reported that homology analysis of the complete amino acid sequences divides the  $\alpha$ -glucosidases into two groups, namely, family I and family II [31,32]. Family I enzymes show higher activity toward heterogeneous substrates such as sucrose and pNPG, and none or less toward homogeneous substrates such as maltooligosaccharides, implying that  $\alpha$ -glucosidase I recognizes the "glucosyl structure" in the substrate. In contrast, family II enzymes hydrolyze homogeneous substrates more rapidly than heterogeneous substrates, indicating that this class of  $\alpha$ -glucosidases recognizes the "maltosyl structure." It has been

reported that family I and II enzymes belong to GH13 and GH31, respectively [33,34]. AgIA is much closer to family II enzyme in terms of substrate specificity; however, the amino acid sequence is somewhat distinct from that of both families. The inhibition patterns of  $\alpha$ -glucosidase-related enzymes from various sources against acarbose were compared (Table 6). Acarbose showed potent inhibitory action toward  $\alpha$ -glucosidases obtained from baker's yeast and rat intestine, CGTase from *Bacillus macerans*, and porcine pancreatic  $\alpha$ -amylase, with competitive-type and mixed-type inhibitions, respectively. For rat intestine  $\alpha$ -glucosidases, the inhibitory potency of acarbose was found to be highest compared to other enzymes. The inhibitory ability of acarbose toward archaeal  $\alpha$ -glucosidase AgIA was between that of yeast and rat intestine  $\alpha$ -glucosidases. For the yeast enzyme, a large  $K_i$  value was obtained for acarbose inhibition compared to that for the intestine enzyme; the ratio being greater than 1000. Since the yeast enzyme belongs to  $\alpha$ -glucosidase family I and the intestinal enzyme belongs to  $\alpha$ -glucosidase family II, there is a possibility that the two analogues are distinctively recognized by the enzymes of the different families.

The transglycosylation property of AgIA was examined using arbutin as an acceptor. AgIA successfully synthesized two distinct arbutin derivatives. Identification of the transglucosylation products AG1 and AG2 revealed that AgIA catalyzed the regioselective formation of glycosidic bonds through an  $\alpha$ -1,6 and  $\alpha$ -1,3-linkages. The formation of  $\alpha$ -1,6 or  $\alpha$ -1,3-linkage is industrially useful for the production of isomaltooligosaccharides and human milk oligosaccharide, such as 3'-sialyllactose, respectively. To the best of our knowledge, the *T. acidophilum*  $\alpha$ -glucosidase described here is the first characterized thermostable archaeal member of the GH31 family, which confirms the transglucosylation activity. Therefore, AgIA which is able to form an  $\alpha$ -1,3-glucosidic linkage as well as  $\alpha$ -1,6-glucosidic linkage should be useful for investigating oligosaccharides and their biological functions and for constructing novel glycoconjugates that will be used in therapeutic applications.

#### Acknowledgement

This work was supported by a Bio-Scientific Research Grant funded by the Pusan National University (PNU, Bio-Scientific Research Grant) (PNU-2008-101-204).

## References

- [1] O. Nashiru, S. Koh, S.-Y. Lee, D.-S. Lee, J. Biochem. Mol. Biol. 34 (2001) 347–354.
- [2] A. Noguchi, M. Yano, Y. Oshima, H. Hemmi, M. Inohara-Ochiai, M. Okada, K.-S. Min, T. Nakayama, T. Nishino, J. Biochem. 134 (2003) 543–550.
- [3] R. Prodanović, N. Milosavić, D. Sladić, M. Zlatović, B. Božić, T. Veličković, Z. Vujčić, J. Mol. Catal. B: Enzym. 35 (2005) 142–146.
- [4] M. Nakao, T. Nakayama, M. Harada, A. Kakudo, H. Ikemoto, S. Kobayashi, Y. Shibano, Appl. Microbiol. Biotechnol. 41 (1994) 337–343.
- [5] N. Kato, S. Suyama, M. Shirokane, M. Kato, T. Kobayashi, N. Tsukagoshi, Appl. Environ. Microbiol. 68 (2002) 1250–1256.
- [6] M. Scigelova, D.H.G. Crout, J. Mol. Catal. B: Enzym. 8 (2000) 175–181.
- [7] T. Nakakuki, J. Appl. Glycosci. 52 (2005) 267–271.
- [8] M. Vihinen, P. Mantsala, Crit. Rev. Biochem. Mol. Biol. 24 (1989) 329–418.
- [9] D.H.C. Crout, P. Critchley, D. Muller, M. Scigelova, S. Singh, G. Vic, in: H.J. Gilbert, G.J. Davies, B. Henrissat, B. Svensson (Eds.), Recent Advances in Carbohydrate Bioengineering, The Royal Society of Chemistry, Cambridge, 1999, pp. 15–23.
- [10] M. Kurimoto, T. Nishimoto, T. Nakada, H. Chaen, S. Fukuda, Y. Tsujisaka, Biosci. Biotechnol. Biochem. 61 (1997) 699–703.
- [11] Y.W. Kim, J.H. Choi, J.W. Kim, C. Park, J.W. Kim, H. Cha, S.B. Lee, B.H. Oh, T.W. Moon, K.H. Park, Appl. Environ. Microbiol. 69 (2003) 4866–4874.
- [12] A. Martino, C. Schiraldi, S. Fusco, I.D. Lerna, T. Costabile, T. Pellicano, M. Marotta, M. Generoso, J. van der Oost, C.W. Sensen, R.L. Charlebois, M. Moracci, M. Rossi, M. De Rosa, J. Mol. Catal. B: Enzym. 11 (2001) 787–794.
- [13] L.D. Unsworth, J. van der Oost, S. Koutsopoulos, FEBS J. 274 (2007) 4044–4056.
- [14] M. Rolfsmeier, P. Blum, J. Bacteriol. 177 (1995) 482–485.
- [15] H.R. Costantino, S.H. Brown, R.M. Kelly, J. Bacteriol. 172 (1990) 3654–3660.
- [16] K. Piller, R.M. Daniel, H.H. Petach, Biochim. Biophys. Acta 1292 (1996) 197–205.
- [17] M. Rolfsmeier, C. Haseltine, E. Bini, A. Clark, P. Blum, J. Bacteriol. 180 (1998) 1287–1295.
- [18] A. Angelov, M. Putyrski, W. Liebl, J. Bacteriol. 188 (2006) 7123–7131.
- [19] M.M. Bradford, Anal. Biochem. 72 (1976) 248–254.
- [20] J.F. Robyt, R. Mukerjee, Carbohydr. Res. 251 (1994) 187–202.
- [21] T.-H. Park, K.-W. Choi, C.-S. Park, S.-B. Lee, H.-Y. Kang, K.-J. Shon, J.-S. Park, J. Cha, Appl. Microbiol. Biotechnol. 69 (2005) 411–422.
- [22] J. Kang, K.-M. Park, K.-H. Choi, C.-S. Park, G.-E. Kim, D. Kim, J. Cha, Enzyme Microb. Technol. 48 (2011) 260–266.
- [23] J.D. Bendtsen, H. Nielsen, G. von Heijne, S. Brunak, J. Mol. Biol. 340 (2004) 783–795.
- [24] K. Buchholz, J. Seibel, in: G. Eggleston, G.L. Gote (Eds.), Oligosaccharides in Food and Agriculture, ACS Symposium Series, vol. 849, American Chemical Society, Washington, DC, 2003, pp. 63–74.
- [25] R.G. Crittenden, M.J. Playne, Trends Food Sci. Technol. 7 (1996) 353–361.
- [26] F. Takenaka, H. Uchiyama, Biosci. Biotechnol. Biochem. 64 (2000) 1821–1826.
- [27] C. Zhou, Y. Xue, Y. Zhang, Y. Zeng, Y. Ma, J. Microbiol. Biotechnol. 19 (2009) 1547–1556.
- [28] V.S. Hung, Y. Hatada, S. Goda, J. Lu, Y. Hidaka, Z. Li, M. Akkita, Y. Ohta, K. Watanabe, H. Matsui, S. Ito, K. Horikoshi, Appl. Microbiol. Biotechnol. 68 (2005) 757–765.
- [29] A.L. Lovering, S.S. Lee, Y.W. Kim, S.G. Withers, N.C. Strynadka, J. Biol. Chem. 280 (2005) 2105–2115.
- [30] E. Serour, G. Antranikian, Anton. Leeuw. 81 (2002) 73–83.
- [31] S. Chiba, Biosci. Biotechnol. Biochem. 61 (1997) 1233–1239.
- [32] A. Kimura, Trends Glycosci. Glycotechnol. 12 (2000) 373–380.
- [33] B. Henrissat, Biochem. J. 280 (1991) 309–316.
- [34] B. Henrissat, A. Bairoch, Biochem. J. 293 (1993) 781–788.
- [35] M.-J. Kim, S.-B. Lee, H.-S. Lee, S.-Y. Lee, J.-S. Baek, D. Kim, T.-W. Moon, J.F. Robyt, K.-H. Park, Arch. Biochem. Biophys. 371 (1999) 277–283.